0νββ-decay nuclear matrix elements in self-consistent Skyrme quasiparticle random-phase approximation: Uncertainty from pairing interaction

W.-L. Lv (吕万里) ,[1,2] Y.-F. Niu (牛一斐) ,[1,2,*] D.-L. Fang (房栋梁) ,[3] J.-M. Yao (尧江明) ,[4]
C.-L. Bai (白春林),[5] and J. Meng (孟杰) [6]

[1]*School of Nuclear Science and Technology, Lanzhou University, Lanzhou 730000, China*
[2]*Frontiers Science Center for Rare isotopes, Lanzhou University, Lanzhou 730000, China*
[3]*Institute of Modern Physics, Chinese Academy of Sciences, Lanzhou 730000, China*
[4]*School of Physics and Astronomy, Sun Yat-sen University, Zhuhai 519082, China*
[5]*Department of Physics, Science, and Technology, Sichuan University, Chengdu 610065, China*
[6]*School of Physics, Peking University, Beijing 100871, China*

The uncertainty in the nuclear matrix elements (NMEs) of $0\nu\beta\beta$ decay for ^{76}Ge, ^{82}Se, ^{128}Te, ^{130}Te, and ^{136}Xe in the self-consistent quasiparticle random phase approximation (QRPA) method is investigated by using eighteen Skyrme interactions supplemented with either a volume or surface type of pairing interactions. The NMEs for the isotopes concerned (except ^{136}Xe) are less sensitive to the particle-hole (ph) interactions, while they are strongly dependent on the employed isovector particle-particle (pp) pairing interactions even though the pairing strengths are optimized to the same pairing gap. The results indicate that a precise determination of the isovector pp pairing interaction in the Skyrme energy density functional is of importance to reduce the uncertainty in the NMEs within the QRPA framework.

Introduction. Neutrinoless double-beta ($0\nu\beta\beta$) decay is a lepton-number-violating process, which is preferred by extensions of the standard model [1–3]. Such a hypothetical second-order transition occurs only if neutrinos are their own antiparticles, i.e., Majorana particles. Besides demonstrating the existence of lepton-number violation, if this process is driven by the standard mechanism of exchange of light Majorana neutrinos, the discovery of $0\nu\beta\beta$ decay provides a practical way to determine the mass scale and mass hierarchy of neutrinos, provided that the corresponding nuclear matrix elements (NMEs) $M^{0\nu}$ are known. Since not only the unknown neutrino properties but also nuclear physics are involved, the NMEs can only be obtained by nuclear many-body approaches; see for instance the recent reviews [4–6], among which the quasiparticle random phase approximation (QRPA) and interacting shell model (ISM) are two widely used microscopic models.

Due to the large discrepancy in the NMEs obtained by different nuclear models, a great deal of effort has been made to reduce this uncertainty. Based on the nuclear models of either ISM [7] or QRPA with G-matrix-based residual interactions (G-QRPA) [8–13], the effects of the induced currents, the size of the single-particle basis, dipole-form-factor cutoff parameters, and short-range correlation have been assessed. In particular, by using different realistic nucleon-nucleon (NN) potentials renormalized by the G matrix, including Bonn, Argonne, and Nijmegen, Rodin *et al.* found that the NMEs

are essentially independent of the residual interactions in the QRPA [9]. However, in their QRPA approach the ground state is obtained by the same Coulomb corrected Woods-Saxon potential, even though the residual interactions for excited states are different [14,15]. Therefore, the uncertainty study of $M^{0\nu}$ using NN interactions needs to be revisited with the self-consistent QRPA, where the same effective NN interactions are consistently used for both the ground state and excited states.

In the past decade, the fully self-consistent QRPA based on Skyrme energy density functionals (EDFs) has been applied to the study of $\beta\beta$ decay. The effects of the overlap factor of excited states, many-body correlations, as well as the isoscalar pairing on $M^{0\nu}$ are studied [16–19]. In Ref. [20], axially deformed Skyrme QRPA was used to calculate $M^{0\nu}$ for the first time. Recently, the NMEs of $2\nu\beta\beta$ decay, $M^{2\nu}$, calculated by deformed Skyrme QRPA using the finite amplitude method [21] and spherical relativistic QRPA [22] became available. In these studies, however, the uncertainty of $M^{0\nu}$ was not investigated.

The aim of this paper is to study the uncertainty of $M^{0\nu}$ induced by the effective interaction. For the particle-hole (ph) channel, focusing on different facets of nuclei, hundreds of Skyrme functionals have been determined [23]. Properties of these Skyrme functionals vary to a large extent, especially the effective mass m^* and the Landau parameter g'_0, which determine the single-particle structure near the Fermi surface and charge-exchange excitations, respectively [24–26]. These two properties are key elements in the calculation of $M^{0\nu}$. Therefore, it is important to investigate the sensitivity

*niuyf@lzu.edu.cn

of NMEs to different Skyrme interactions. For the particle-particle (pp) channel, it has been found that $M^{0\nu}$ is sensitive to pairing energies. By analyzing the angular momentum of the two decaying neutrons, the contributions of $\mathcal{J} = 0$ pairs to the NMEs, determined by the isovector pairing, are always found to be positive [11,27]. By calculating the NME as a function of the intrinsic deformation of ^{150}Nd and ^{150}Sm and the NMEs in the cadmium isotopic chain $^{98-132}$Cd, the authors demonstrate that the NMEs will be enhanced if there is a large amount of pairing correlations [28,29]. In both spherical and axially deformed Skyrme QRPA, volume pairing is always used [16–21]. It is worth mentioning that in Skyrme QRPA calculations for nuclear excitations, the surface pairing has also been commonly utilized [30–32] and there is no definitive proof that indicates a preference for volume pairing over surface pairing, or vice versa [33]. Especially, the influence on the NME values of the character of pairing correlations is unknown. Therefore, it becomes especially intriguing to quantify the uncertainty that arises from selecting different pairing interactions in QRPA calculations of NMEs for $0\nu\beta\beta$ decay.

Formalism. In the self-consistent QRPA, the same effective nuclear interaction is employed to solve the Hartree-Fock-Bogoliubov (HFB) equation and the followup QRPA equation. For the ph channel, we use the Skyrme interaction. For the pp channel, we use the δ interaction [33,34],

$$V^{\text{pp}}(\boldsymbol{r}_1, \boldsymbol{r}_2) = \left[t_0' + \frac{t_3'}{6} \rho \left(\frac{\boldsymbol{r}_1 + \boldsymbol{r}_2}{2} \right) \right] \delta(\boldsymbol{r}_1 - \boldsymbol{r}_2), \quad (1)$$

which corresponds to the surface or volume type of pairing interactions when the t_3' term is switched on or off. In the case of surface pairing, $t_3' = -37.5t_0'$ is employed, where the pairing field is peaked at the nuclear surface and follows roughly the variations of the nucleon density.

The nuclear matrix element of $0\nu\beta\beta$ decay is defined as

$$M^{0\nu} \equiv -M_{\text{F}}^{0\nu} + M_{\text{GT}}^{0\nu} + M_{\text{T}}^{0\nu}, \quad (2)$$

where the tensor term $M_{\text{T}}^{0\nu}$ is negligibly small [8,20]. For the ground-state-to-ground-state transition ($0_{\text{g.s.}}^{(i)+} \rightarrow 0_{\text{g.s.}}^{(f)+}$),

$$M_K^{0\nu} = \frac{8R}{g_A^2} \int q^2 dq \sum_{N_i N_f} \sum_{J^P} \sum_{\pi_i \nu_i} \sum_{\pi_f \nu_f} \frac{1}{(2J+1)} \frac{h_K(q^2)}{q(q+E_d)}$$
$$\times \langle 0_{\text{g.s.}}^{(f)+} || [c_{\pi_f}^\dagger \tilde{c}_{\nu_f}]_J || N_f J^P \rangle \langle N_f J^P | N_i J^P \rangle$$
$$\times \langle N_i J^P || [c_{\pi_i}^\dagger \tilde{c}_{\nu_i}]_J || 0_{\text{g.s.}}^{(i)+} \rangle$$
$$\times S_K \langle j_{\pi_f} || \hat{O}_K || j_{\nu_f} \rangle \langle j_{\pi_i} || \hat{O}_K || j_{\nu_i} \rangle. \quad (3)$$

The form factors h_K ($K = \text{F, GT}$) take into account the nucleon finite size and higher order currents [8]. For the Fermi term, $S_{\text{F}} = (-)^J$ and $\hat{O}_{\text{F}} = j_J(qr)Y_J$. For the GT (Gamow-Teller) term, $S_{\text{GT}} = \sum_{l=J-1}^{J+1}(-)^l$ and $\hat{O}_{\text{GT}} = j_l(qr)[Y_l \sigma]_J$. Here $j_k(qr)$ is the spherical Bessel function of kth order and Y_k is the spherical harmonic function. An empirical formula of the nuclear radius is adopted, i.e., $R = 1.2A^{1/3}$ fm. In QRPA model, the closure approximation can be avoided, $E_d = (\Omega_{N_i} + \Omega_{N_f} + \Delta\lambda_{\pi\nu}^{(i)} - \Delta\lambda_{\pi\nu}^{(f)})/2$, where Ω_{N_i} (Ω_{N_f}) and $\Delta\lambda_{\pi\nu}^{(i)}$ ($\Delta\lambda_{\pi\nu}^{(f)}$) are respectively the eigenvalues of QRPA
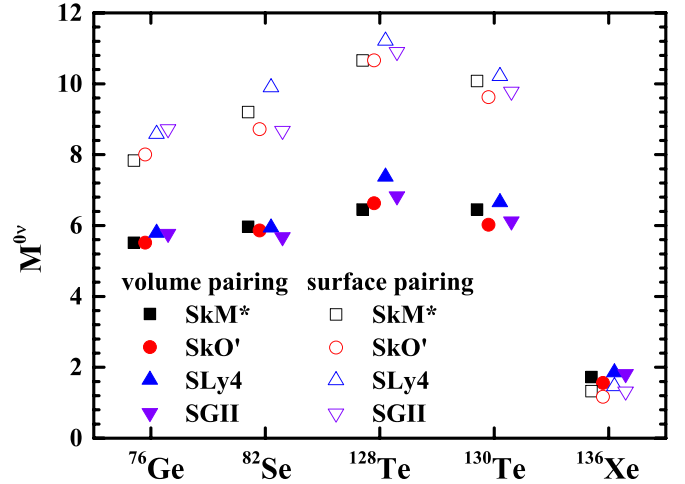

FIG. 1. $M^{0\nu}$ for ^{76}Ge, ^{82}Se, ^{128}Te, ^{130}Te, and ^{136}Xe, calculated by self-consistent QRPA model with four Skyrme interactions (denoted by different shapes of symbols) and two kinds of pairing interactions (denoted by solid symbols for volume pairing and hollow symbols for surface pairing).

equation and the difference of proton and neutron Fermi surfaces for mother (daughter) nucleus (cf. Eq. (10) in Ref. [35]). $\langle N_f J^P | N_i J^P \rangle$ is the overlap factor of the two QRPA excited states [15].

Results and discussions. In Skyrme HFB calculations, the pairing (neutron-neutron and proton-proton) interactions are fixed to reproduce the experimental pairing gaps obtained from three-point formula of binding energies. For the residual pairing interactions in QRPA, the strengths of isoscalar proton-neutron pairing f_{IS} are fixed by tuning $M_{\text{GT}}^{2\nu}$ to the experimental data [36], while the strengths of isovector channel f_{IV} are determined by $M_{\text{F}}^{2\nu} = 0$ due to the isospin symmetry [37]. Intermediate states of $J^P = 0^\pm$–$10^\pm$ are considered. An unquenched value of axial-vector coupling constant $g_A = 1.27$ is used. The modifications on the time-odd spin-isospin coupling constants of the Skyrme functionals [20,25,38,39] are not adopted in our calculations in order to keep the self-consistency of our model calculation since these time-odd constants are already determined by Skyrme force parameters. With these consistently obtained time-odd parameters, the agreement between theoretical GT centroid energy and the experimental one is also reasonable. Since we focus on the uncertainty of NME induced by pairing, we treat all the nuclei as spherical ones to simplify the problem, and our conclusion also holds after deformation effects are considered.

We first perform a systematic calculation on the NMEs of $0\nu\beta\beta$ for ^{76}Ge, ^{82}Se, ^{128}Te, ^{130}Te, and ^{136}Xe, where SkM* [40], SkO' [41], SLy4 [42], and SGII [43] interactions are used for the ph channel. The tensor force is not included in this work. Both volume and surface pairing interactions are used for the pp channel. Results are depicted in Fig. 1. One can see clearly that with the same kind of pairing interaction, $M^{0\nu}$ obtained by different ph interactions are close to each other, with the discrepancy less than 15% for all the nuclei of concerned. However, $M^{0\nu}$ is sensitive to the use of pairing interactions. The use of the surface pairing interaction leads
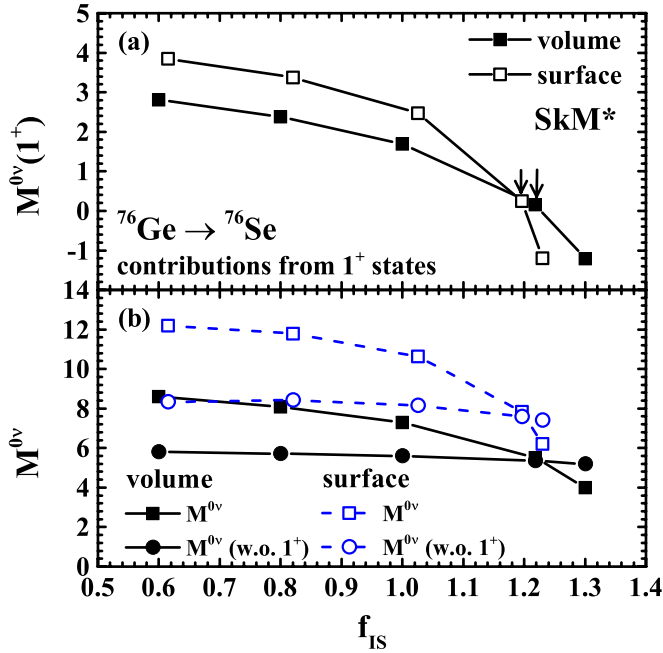
FIG. 2. $M^{0\nu}$ for ^{76}Ge as a function of the isoscalar pairing strength f_{IS}. The contributions to $M^{0\nu}$ from 1^+ intermediate states are shown in panel (a), where the arrows mark the f_{IS} fixed by experimental $M^{2\nu}_{GT}$. The total values and the values without the contributions from 1^+ intermediate states of $M^{0\nu}$ are shown in panel (b).

to a much larger $M^{0\nu}$ than the use of volume pairing, except for ^{136}Xe.

To understand the difference of $M^{0\nu}$ between volume pairing and surface pairing, we plot in Fig. 2 the $M^{0\nu}$ for ^{76}Ge as a function of the isoscalar pairing strength f_{IS}. The contribution from 1^+ states to $M^{0\nu}$, denoted as $M^{0\nu}(1^+)$ shown in Fig. 2(a), decreases rapidly with increasing f_{IS}, which is similar to the trend of NMEs of $2\nu\beta\beta$ decay $M^{2\nu}_{GT}$ [35]. It comes from the fact that, for both $M^{0\nu}(1^+)$ and $M^{2\nu}_{GT}$, only 1^+ intermediate states are involved, which are sensitive to isoscalar pairing. By adjusting the value of f_{IS} to reproduce the experimental $M^{2\nu}_{GT}$ in the calculations, the values of $M^{0\nu}(1^+)$ by the volume and surface pairing interactions are close to each other. However, unlike 1^+ states, other multipoles are not so sensitive to isoscalar pairing so that their contributions to $M^{0\nu}$ are stable for different f_{IS}, as shown in panel (b). As a result, the behavior of the total $M^{0\nu}$ mainly depends on the the decreasing trend of $M^{0\nu}(1^+)$ when increasing f_{IS}, while the difference of $M^{0\nu}$ between volume pairing and surface pairing comes from the different contributions of other multipoles in these two cases. Since $M^{0\nu}$ contributed by other multipoles is not sensitive to isoscalar pairing, the difference in the $M^{0\nu}$ from the different form of pairing interaction should be caused by the isovector pairing part.

In the calculation of $M^{0\nu}$, pairing interaction plays its role mainly through the overlap of HFB wave functions $\langle\text{HFB}_f|\text{HFB}_i\rangle$, one-body transition densities, as well as the number of two-quasiparticle (2qp) proton-neutron configurations. To qualitatively investigate the pairing effects on $M^{0\nu}$, we introduce the sum of one-body transition densities δ_{NJ^P},
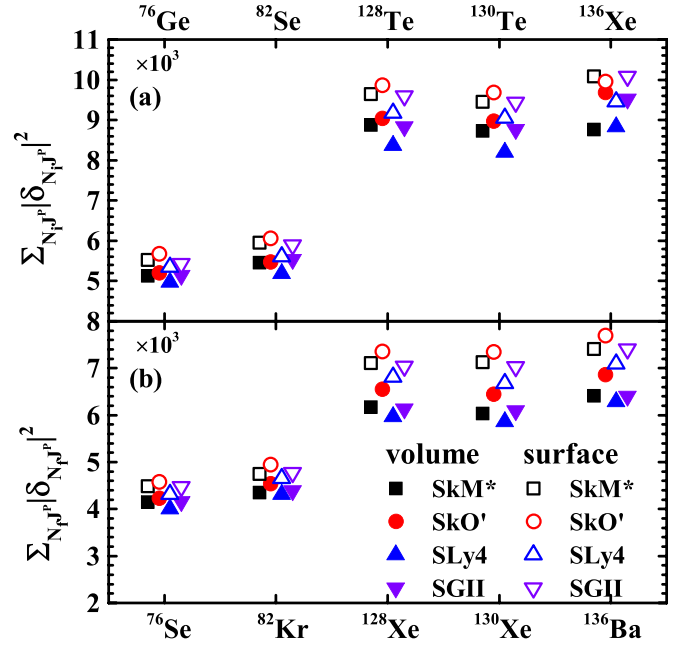

FIG. 3. $\sum_{NJ^P}|\delta_{NJ^P}|^2$ in mother nuclei (a) and in daughter nuclei (b).

defined as

$$\delta_{N_iJ^P} \equiv -(2J+1)^{-1/2}\sum_{\pi_i\nu_i}\langle N_iJ^P||[c^\dagger_{\pi_i}\tilde{c}_{\nu_i}]_J||0^{(i)+}_{\text{g.s.}}\rangle,$$

$$\delta_{N_fJ^P} \equiv -(2J+1)^{-1/2}\sum_{\pi_f\nu_f}\langle 0^{(f)+}_{\text{g.s.}}||[c^\dagger_{\pi_f}\tilde{c}_{\nu_f}]_J||N_fJ^P\rangle, \quad (4)$$

where the number of 2qp configurations of QRPA is considered by $\sum_{\pi\nu}$ and the occupation amplitudes are involved in one-body transition densities, $\langle N_iJ^P||[c^\dagger_{\pi_i}\tilde{c}_{\nu_i}]_J||0^{(i)+}_{\text{g.s.}}\rangle$ and $\langle 0^{(f)+}_{\text{g.s.}}||[c^\dagger_{\pi_f}\tilde{c}_{\nu_f}]_J||N_fJ^P\rangle$. In Fig. 3, we compare the sum of $|\delta_{NJ^P}|^2$ for both mother and daughter nuclei of $\beta\beta$ decay. With the same kind of pairing, $\sum_{NJ^P}|\delta_{NJ^P}|^2$ for different Skyrme interactions are similar. However, for each Skyrme interaction, $\sum_{NJ^P}|\delta_{NJ^P}|^2$ obtained by the surface pairing is always larger than that obtained by the volume pairing. We notice that although the mean pairing gaps determined by the isovector pairing for the ground-state calculation are fixed to the experimental data, the occupations of single-particle levels around the Fermi surface are very different for volume-pairing and surface-pairing cases. In the case of the volume pairing, the distribution of occupation probability is much sharper than the case of surface pairing. As a result, there are more single-particle levels with partial occupations for the case of surface pairing, and this will lead to a larger 2qp space for QRPA calculation, and hence a larger $\sum_{NJ^P}|\delta_{NJ^P}|^2$ value, which immediately gives rise to a larger $M^{0\nu}$ when using surface pairing.

The values of the overlaps $\langle\text{HFB}_f|\text{HFB}_i\rangle$ are similar for different pairing interactions for all considered nuclei, around 0.82, except for the semimagic nucleus ^{136}Xe, whose values are around 0.45 and 0.25 for the cases of volume pairing and surface pairing, respectively. This is because a sharper
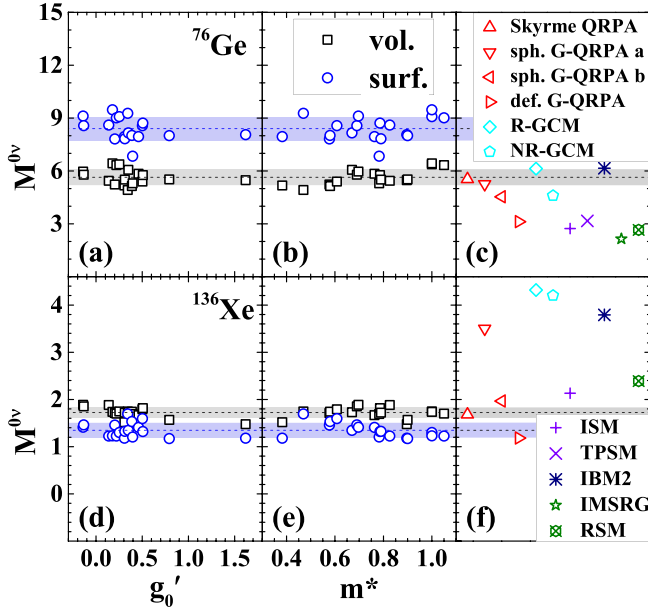
FIG. 4. $M^{0\nu}$ for ^{76}Ge [panels (a) and (b)] and ^{136}Xe [panels (d) and (e)] with 18 Skyrme interactions and two kinds of pairing interactions. Black squares and blue circles are respectively the results of volume and surface pairing interactions. Their corresponding mean values and standard deviations are represented by the dashed lines and shaded regions. Results of other nuclear models for ^{76}Ge and ^{136}Xe are plotted in panels (c) and (f), respectively.

distribution of the occupation probability for neutrons in the daughter nucleus ^{136}Ba in the case of volume pairing is more similar to that in the mother nucleus ^{136}Xe, which is a step function due to the magic neutron number. As a result, although the $\sum_{NJ^P} |\delta_{NJ^P}|^2$ in ^{136}Xe is not different from other nuclei, by considering the overlap factor $\langle \text{HFB}_f | \text{HFB}_i \rangle$ for ^{136}Xe, the $M^{0\nu}$ by different pairing interactions are similar, where volume pairing even gives a slightly larger $M^{0\nu}$ compared to the surface pairing case, as shown in Fig. 1.

Since ^{76}Ge and ^{136}Xe are of experimental interest to GERDA [44] and MAJORANA [45] Collaborations and to EXO [46], KamLAND-Zen [47], and XENON [48] Collaborations, we further systematically examine the independence on ph channel interaction and dependence on ground-state isovector pp interaction of $M^{0\nu}$ for ^{76}Ge and ^{136}Xe. Besides the previously used SkM*, SkO', SLy4, and SGII, another 14 Skyrme interactions are employed. They are SLy5 [42], SKO [41], SGI [43], SII, SIII, SIV [49], LNS [50], SkT6 [51], BSk1 [52], MSk1 [53], SkI3, SkI4 [54], SAMi [55], and Z_σ [56]. The effective mass m^* and Landau parameter g_0' of these interactions span a wide range. The former will affect the structure of single-particle levels [24], while the later plays an important role in spin-isospin excitations [25]. Results of $M^{0\nu}$ with 18 Skyrme interactions and two kinds of pairing forces are depicted in Fig. 4. Their mean values $\overline{M}^{0\nu}$ and standard deviations σ are listed in Table I. For each kind of pp interaction, $M^{0\nu}$ obtained by different ph interactions are close, where the standard deviations σ are only around 10% of the mean values $\overline{M}^{0\nu}$. Besides, as shown in Fig. 1, $M^{0\nu}$

TABLE I. Mean values $\overline{M}^{0\nu}$ and the standard deviation σ of $M^{0\nu}$ obtained by 18 Skyrme interactions and two kinds of pairing interactions for ^{76}Ge and ^{136}Xe.

Nucleus	Volume pairing		Surface pairing	
	^{76}Ge	^{136}Xe	^{76}Ge	^{136}Xe
$\overline{M}^{0\nu}$	5.65	1.72	8.40	1.35
σ of $M^{0\nu}$	0.45	0.11	0.66	0.15

obtained by volume pairing are generally smaller for the open shell nucleus ^{76}Ge and larger for semimagic nucleus ^{136}Xe due to the occupation probability distribution around Fermi surface.

We further make a brief comparison of the NMEs between our values and other theoretical results in Figs. 4(c) and 4(f). For ^{76}Ge, our value of the NME is 5.65(45) in the case of volume pairing, which is very close to the previous Skyrme QRPA calculation [20]. Also, the NMEs obtained by spherical G-QRPA [57,58], relativistic (R) and nonrelativistic (NR) generator coordinate methods (GCM) [28,59], and the interacting boson model (IBM2) [60] lie within around 1.0σ–2.0σ from our $\overline{M}^{0\nu}$ by volume pairing, while our results are about twice the NMEs obtained by the deformed G-QRPA [61], ISM [7], triaxial projected shell model (TPSM) [62], and *ab initio* approaches including in-medium similarity renormalization group (IMSRG) [63] and realistic shell model (RSM) [64], which could be caused by the lack of complicated many-body correlations [5,11]. For ^{136}Xe, our values of the NMEs are 1.72(11) by the volume pairing and 1.35(15) by the surface pairing, which are respectively close to the results of previous Skyrme QRPA and deformed G-QRPA. Either by the volume pairing or surface pairing, our results are smaller than the other models. The reason could be the sharp neutron Fermi surface in ^{136}Xe [20], which significantly suppresses the NMEs through the overlap of HFB functions.

We make some attempts to distinguish which type of pairing is more favored. For both mother and daughter nuclei of ^{76}Ge and ^{136}Xe decays, the $B(E2; 0^+_{\text{g.s.}} \to 2^+_1)$ values can be better reproduced by volume pairing compared to surface pairing. However, the average $Q_{\beta\beta}$ values of 18 Skyrme functionals are closer to the experimental ones in the case of surface pairing. Since the experimental occupation numbers [66–71] have been used to improve the calculations of NMEs [72–74], we also compare the theoretical values by Skyrme HFB to them. Generally, the performances of the two parings are similar. We also perform a test calculation using experimental occupancies to compute the NMEs for ^{76}Ge and ^{136}Xe. However, the changes on NMEs are only about 1–5 % for ^{76}Ge and 5–17 % for ^{136}Xe. Properties of spin-isospin resonances are important for $\beta\beta$ decays [75–78]. For the centroid energies of GTGR, the performance of surface pairing is a little bit better. By applying the pairing strengths optimized by the experimental mean pairing gaps in the even-even nuclei, we calculate the binding energies of their odd-even neighbors in order to compute the theoretical mean pairing gaps with the three-point formula. The surface pairing seems better for ^{76}Ge
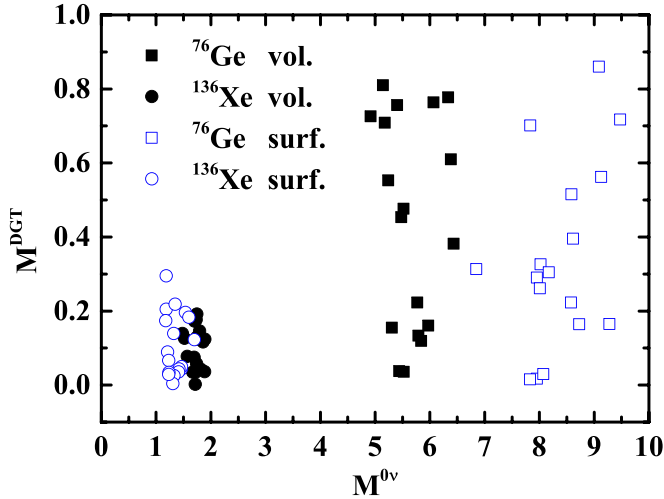
FIG. 5. Double GT matrix elements M^{DGT} versus $M^{0\nu}$. Results are for two nuclei, ^{76}Ge (square) and ^{136}Xe (circle), obtained by 18 Skyrme interactions and two kinds of pairing interactions, where solid and hollow symbols are respectively the results of volume and surface pairing interactions.

and worse for ^{76}Se, and ^{136}Xe. The pairing gaps are always overestimated by the surface pairing, while they are usually underestimated by the volume pairing, which implies there are more pairing correlations when using surface pairing. Such a result is consistent with the magnitudes of NMEs and earlier findings [11,27–29]. In conclusion, there is no compelling argument for favoring one type of pairing over the other.

In view of the recent interest in the study of the possible correlation between the matrix elements of double Gamow-Teller transition M^{DGT} and $M^{0\nu}$ [58,65,79], we examine this correlation with the QRPA using 18 Skyrme interactions in Fig. 5. In contrast to the independence of ph interaction in $M^{0\nu}$, M^{DGT} is strongly affected by the choice of ph interactions. Consequently, there seems to be no correlation between M^{DGT} and $M^{0\nu}$ in the QRPA model. The reason could be the different behaviors of the distributions of M^{DGT} and $M^{0\nu}$ as functions of the internucleon distance r in QRPA. Both the short range region ($r \lesssim 3$fm) and long range region ($r \gtrsim 3$fm) contribute much to M^{DGT}, while only the short range region governs $M^{0\nu}$ [58,79,80].

Conclusions and perspectives. In summary, the dependence of NMEs of $0\nu\beta\beta$ decay on ph and pp interactions is inves-

tigated in the framework of self-consistent QRPA based on Skyrme density functionals. Similar values for the $M^{0\nu}$ are obtained by different Skyrme interactions, namely, ph interactions. In the systematical calculations of $\beta\beta$ emitters ^{76}Ge and ^{136}Xe with 18 Skyrme interactions having a large span over Landau parameter and effective mass, standard deviations are only around 10% of the mean values $\overline{M}^{0\nu}$. However, $M^{0\nu}$ shows a dependence on pp interaction. For open shell nuclei ^{76}Ge, ^{82}Se, ^{128}Te, and ^{130}Te, $M^{0\nu}$ obtained by surface pairing are always much larger than those obtained by volume pairing, due to the bigger 2qp space of the QRPA model caused by a more smeared occupation probability distribution. The inverse case is found in the semimagic nucleus ^{136}Xe with much closer results, caused by the different situation in the calculation of overlap factor $\langle HFB_f | HFB_i \rangle$, where the sharp occupation probability distribution given by the volume pairing gives a larger value. We also investigate the correlation between M^{DGT} and $M^{0\nu}$. Due to the dependence of M^{DGT} on the ph interaction, there seems no correlation between them.

In the case of volume pairing, the NMEs for ^{76}Ge and ^{136}Xe are respectively 5.65(45) and 1.72(11), while in the case of surface pairing they are 8.40(66) and 1.35(15). The large uncertainty originates from the isovector pairing interaction, which cannot be uniquely determined by the pairing gaps. Therefore, other constraints on the pairing interactions need to be considered in order to reduce the observed uncertainty in the NMEs by the QRPA method.

[1] F. T. Avignone, S. R. Elliott, and J. Engel, Rev. Mod. Phys. **80**, 481 (2008).

[2] H. Ejiri, J. Suhonen, and K. Zuber, Phys. Rep. **797**, 1 (2019).

[3] M. J. Dolinski, A. W. Poon, and W. Rodejohann, Annu. Rev. Nucl. Part. Sci. **69**, 219 (2019).

[4] J. D. Vergados, H. Ejiri, and F. Šimkovic, Rep. Prog. Phys. **75**, 106301 (2012).

[5] J. Engel and J. Menéndez, Rep. Prog. Phys. **80**, 046301 (2017).

[6] J. M. Yao, J. Meng, Y. F. Niu, and P. Ring, Prog. Part. Nucl. Phys. **126**, 103965 (2022).

[7] J. Menéndez, A. Poves, E. Caurier, and F. Nowacki, Nucl. Phys. A **818**, 139 (2009).

[8] F. Šimkovic, G. Pantis, J. D. Vergados, and A. Faessler, Phys. Rev. C **60**, 055502 (1999).

[9] V. A. Rodin, A. Faessler, F. Šimkovic, and P. Vogel, Phys. Rev. C **68**, 044302 (2003).

[10] V. A. Rodin, A. Faessler, F. Šimkovic, and P. Vogel, Nucl. Phys. A **766**, 107 (2006).

[11] F. Šimkovic, A. Faessler, V. Rodin, P. Vogel, and J. Engel, Phys. Rev. C **77**, 045503 (2008).

[12] M. Kortelainen and J. Suhonen, Phys. Rev. C **76**, 024315 (2007).

[13] J. Suhonen and M. Kortelainen, Int. J. Mod. Phys. E **17**, 1 (2008).

[14] D. L. Fang, Neutrinoless double beta decay in deformed nuclei: Its implications in particle and nuclear physics, Ph.D. thesis, Universität Tübingen, 2011 (unpublished).

[15] F. Šimkovic, L. Pacearescu, and A. Faessler, Nucl. Phys. A **733**, 321 (2004).

[16] J. Terasaki, Phys. Rev. C **86**, 021301(R) (2012).

[17] J. Terasaki, Phys. Rev. C **91**, 034318 (2015).

[18] J. Terasaki and Y. Iwata, Phys. Rev. C **100**, 034325 (2019).

[19] J. Terasaki, Phys. Rev. C **102**, 044303 (2020).

[20] M. T. Mustonen and J. Engel, Phys. Rev. C **87**, 064302 (2013).

[21] N. Hinohara and J. Engel, Phys. Rev. C **105**, 044314 (2022).

[22] N. Popara, A. Ravlić, and N. Paar, Phys. Rev. C **105**, 064315 (2022).

[23] M. Dutra, O. Lourenço, J. S. Sá Martins, A. Delfino, J. R. Stone, and P. D. Stevenson, Phys. Rev. C **85**, 035201 (2012).

[24] D. Vautherin and D. M. Brink, Phys. Rev. C **5**, 626 (1972).

[25] S. Fracasso and G. Colò, Phys. Rev. C **76**, 044307 (2007).

[26] Y. F. Niu, G. Colò, M. Brenna, P. F. Bortignon, and J. Meng, Phys. Rev. C **85**, 034314 (2012).

[27] E. Caurier, J. Menéndez, F. Nowacki, and A. Poves, Phys. Rev. Lett. **100**, 052503 (2008).

[28] T. R. Rodríguez and G. Martínez-Pinedo, Phys. Rev. Lett. **105**, 252503 (2010).

[29] T. R. Rodríguez and G. Martínez-Pinedo, Phys. Lett. B **719**, 174 (2013).

[30] J. Li, G. Colò, and J. Meng, Phys. Rev. C **78**, 064304 (2008).

[31] E. Khan, Phys. Rev. C **80**, 011307(R) (2009).

[32] P. Avogadro and C. A. Bertulani, Phys. Rev. C **88**, 044319 (2013).

[33] J. Dobaczewski, W. Nazarewicz, and M. V. Stoitsov, Eur. Phys. J. A **15**, 21 (2002).

[34] K. Bennaceur and J. Dobaczewski, Comput. Phys. Commun. **168**, 96 (2005).

[35] W. L. Lv, Y. F. Niu, D. L. Fang, and C. L. Bai, Phys. Rev. C **105**, 044331 (2022).

[36] A. S. Barabash, Nucl. Phys. A **935**, 52 (2015).

[37] V. Rodin and A. Faessler, Phys. Rev. C **84**, 014322 (2011).

[38] M. Bender, J. Dobaczewski, J. Engel, and W. Nazarewicz, Phys. Rev. C **65**, 054322 (2002).

[39] T. Shafer, J. Engel, C. Fröhlich, G. C. McLaughlin, M. Mumpower, and R. Surman, Phys. Rev. C **94**, 055802 (2016).

[40] J. Bartel, P. Quentin, M. Brack, C. Guet, and H.-B. Håkansson, Nucl. Phys. A **386**, 79 (1982).

[41] P.-G. Reinhard, D. J. Dean, W. Nazarewicz, J. Dobaczewski, J. A. Maruhn, and M. R. Strayer, Phys. Rev. C **60**, 014316 (1999).

[42] E. Chabanat, P. Bonche, P. Haensel, J. Meyer, and R. Schaeffer, Nucl. Phys. A **635**, 231 (1998).

[43] N. V. Giai and H. Sagawa, Phys. Lett. B **106**, 379 (1981).

[44] M. Agostini, G. R. Araujo, A. M. Bakalyarov, M. Balata, I. Barabanov, L. Baudis, C. Bauer, E. Bellotti, S. Belogurov, A. Bettini, L. Bezrukov, V. Biancacci, D. Borowicz, E. Bossio, V. Bothe, V. Brudanin, R. Brugnera, A. Caldwell, C. Cattadori, A. Chernogorov *et al.* (GERDA Collaboration), Phys. Rev. Lett. **125**, 252502 (2020).

[45] C. E. Aalseth, N. Abgrall, E. Aguayo, S. I. Alvis, M. Amman, I. J. Arnquist, F. T. Avignone, H. O. Back, A. S. Barabash, P. S. Barbeau, C. J. Barton, P. J. Barton, F. E. Bertrand, T. Bode, B. Bos, M. Boswell, A. W. Bradley, R. L. Brodzinski, V. Brudanin, M. Busch *et al.* (Majorana Collaboration), Phys. Rev. Lett. **120**, 132502 (2018).

[46] G. Anton, I. Badhrees, P. S. Barbeau, D. Beck, V. Belov, T. Bhatta, M. Breidenbach, T. Brunner, G. F. Cao, W. R. Cen, C. Chambers, B. Cleveland, M. Coon, A. Craycraft, T. Daniels, M. Danilov, L. Darroch, S. J. Daugherty, J. Davis, S. Delaquis *et al.* (EXO-200 Collaboration), Phys. Rev. Lett. **123**, 161802 (2019).

[47] A. Gando, Y. Gando, T. Hachiya, M. Ha Minh, S. Hayashida, Y. Honda, K. Hosokawa, H. Ikeda, K. Inoue, K. Ishidoshiro, Y. Kamei, K. Kamizawa, T. Kinoshita, M. Koga, S. Matsuda, T. Mitsui, K. Nakamura, A. Ono, N. Ota, S. Otsuka *et al.* (KamLAND-Zen Collaboration), Phys. Rev. Lett. **122**, 192501 (2019).

[48] E. Aprile, K. Abe, F. Agostini, S. Ahmed Maouloud, M. Alfonsi, L. Althueser, B. Andrieu, E. Angelino, J. R. Angevaare, V. C. Antochi, D. Antón Martin, F. Arneodo, L. Baudis, A. L. Baxter, L. Bellagamba, R. Biondi, A. Bismark, A. Brown, S. Bruenner, G. Bruno *et al.* (XENON Collaboration), Phys. Rev. C **106**, 024328 (2022).

[49] M. Beiner, H. Flocard, N. V. Giai, and P. Quentin, Nucl. Phys. A **238**, 29 (1975).

[50] L. G. Cao, U. Lombardo, C. W. Shen, and N. V. Giai, Phys. Rev. C **73**, 014313 (2006).

[51] F. Tondeur, M. Brack, M. Farine, and J. Pearson, Nucl. Phys. A **420**, 297 (1984).

[52] M. Samyn, S. Goriely, P.-H. Heenen, J. Pearson, and F. Tondeur, Nucl. Phys. A **700**, 142 (2002).

[53] F. Tondeur, S. Goriely, J. M. Pearson, and M. Onsi, Phys. Rev. C **62**, 024308 (2000).

[54] P.-G. Reinhard and H. Flocard, Nucl. Phys. A **584**, 467 (1995).

[55] X. Roca-Maza, G. Colò, and H. Sagawa, Phys. Rev. C **86**, 031306(R) (2012).

[56] J. Friedrich and P.-G. Reinhard, Phys. Rev. C **33**, 335 (1986).

[57] J. Hyvärinen and J. Suhonen, Phys. Rev. C **91**, 024613 (2015).

[58] F. Šimkovic, A. Smetana, and P. Vogel, Phys. Rev. C **98**, 064325 (2018).

[59] J. M. Yao, L. S. Song, K. Hagino, P. Ring, and J. Meng, Phys. Rev. C **91**, 024316 (2015).

[60] J. Barea, J. Kotila, and F. Iachello, Phys. Rev. C **87**, 014315 (2013).

[61] D.-L. Fang, A. Faessler, and F. Šimkovic, Phys. Rev. C **97**, 045503 (2018).

[62] Y. K. Wang, P. W. Zhao, and J. Meng, Phys. Rev. C **104**, 014320 (2021).

[63] A. Belley, C. G. Payne, S. R. Stroberg, T. Miyagi, and J. D. Holt, Phys. Rev. Lett. **126**, 042502 (2021).

[64] L. Coraggio, A. Gargano, N. Itaco, R. Mancino, and F. Nowacki, Phys. Rev. C **101**, 044315 (2020).

[65] J. M. Yao, I. Ginnett, A. Belley, T. Miyagi, R. Wirth, S. Bogner, J. Engel, H. Hergert, J. D. Holt, and S. R. Stroberg, Phys. Rev. C **106**, 014315 (2022).

[66] J. P. Schiffer, S. J. Freeman, J. A. Clark, C. Deibel, C. R. Fitzpatrick, S. Gros, A. Heinz, D. Hirata, C. L. Jiang, B. P. Kay, A. Parikh, P. D. Parker, K. E. Rehm, A. C. C. Villari, V. Werner, and C. Wrede, Phys. Rev. Lett. **100**, 112501 (2008).

[67] S. J. Freeman and J. P. Schiffer, J. Phys. G: Nucl. Part. Phys. **39**, 124004 (2012).

[68] B. P. Kay, T. Bloxham, S. A. McAllister, J. A. Clark, C. M. Deibel, S. J. Freedman, S. J. Freeman, K. Han, A. M. Howard, A. J. Mitchell, P. D. Parker, J. P. Schiffer, D. K. Sharp, and J. S. Thomas, Phys. Rev. C **87**, 011302(R) (2013).

[69] J. P. Entwisle, B. P. Kay, A. Tamii, S. Adachi, N. Aoi, J. A. Clark, S. J. Freeman, H. Fujita, Y. Fujita, T. Furuno, T. Hashimoto, C. R. Hoffman, E. Ideguchi, T. Ito, C. Iwamoto, T. Kawabata, B. Liu, M. Miura, H. J. Ong, J. P. Schiffer *et al.*, Phys. Rev. C **93**, 064312 (2016).

[70] S. V. Szwec, B. P. Kay, T. E. Cocolios, J. P. Entwisle, S. J. Freeman, L. P. Gaffney, V. Guimarães, F. Hammache, P. P. McKee, E. Parr, C. Portail, J. P. Schiffer, N. de Séréville, D. K. Sharp, J. F. Smith, and I. Stefan, Phys. Rev. C **94**, 054314 (2016).

[71] S. J. Freeman, D. K. Sharp, S. A. McAllister, B. P. Kay, C. M. Deibel, T. Faestermann, R. Hertenberger, A. J. Mitchell, J. P. Schiffer, S. V. Szwec, J. S. Thomas, and H.-F. Wirth, Phys. Rev. C **96**, 054325 (2017).

[72] J. Suhonen and O. Civitarese, Phys. Lett. B **668**, 277 (2008).

[73] F. Šimkovic, A. Faessler, and P. Vogel, Phys. Rev. C **79**, 015502 (2009).

[74] F. F. Deppisch, L. Graf, F. Iachello, and J. Kotila, Phys. Rev. D **102**, 095016 (2020).

[75] R. Madey, B. S. Flanders, B. D. Anderson, A. R. Baldwin, J. W. Watson, S. M. Austin, C. C. Foster, H. V. Klapdor, and K. Grotz, Phys. Rev. C **40**, 540 (1989).

[76] P. Puppe, D. Frekers, T. Adachi, H. Akimune, N. Aoi, B. Bilgier, H. Ejiri, H. Fujita, Y. Fujita, M. Fujiwara, E. Ganioğlu, M. N. Harakeh, K. Hatanaka, M. Holl, H. C. Kozer, J. Lee, A. Lennarz, H. Matsubara, K. Miki, S. E. A. Orrigo, T. Suzuki, A. Tamii, and J. H. Thies, Phys. Rev. C **84**, 051305(R) (2011).

[77] J. H. Thies, D. Frekers, T. Adachi, M. Dozono, H. Ejiri, H. Fujita, Y. Fujita, M. Fujiwara, E.-W. Grewe, K. Hatanaka, P. Heinrichs, D. Ishikawa, N. T. Khai, A. Lennarz, H. Matsubara, H. Okamura, Y. Y. Oo, P. Puppe, T. Ruhe, K. Suda, A. Tamii, H. P. Yoshida, and R. G. T. Zegers, Phys. Rev. C **86**, 014304 (2012).

[78] P. Puppe, A. Lennarz, T. Adachi, H. Akimune, H. Ejiri, D. Frekers, H. Fujita, Y. Fujita, M. Fujiwara, E. Ganioğlu, E.-W. Grewe, K. Hatanaka, R. Hodak, C. Iwamoto, N. T. Khai, A. Okamoto, H. Okamura, P. P. Povinec, G. Susoy, T. Suzuki, A. Tamii, J. H. Thies, and M. Yosoi, Phys. Rev. C **86**, 044603 (2012).

[79] N. Shimizu, J. Menéndez, and K. Yako, Phys. Rev. Lett. **120**, 142502 (2018).

[80] F. Šimkovic, R. Hodák, A. Faessler, and P. Vogel, Phys. Rev. C **83**, 015502 (2011).